The 2013 World Congress on
Advances in Structural Engineering and Mechanics (ASEM13)
Jeju, Korea, September 8-12, 2013

Effect of fatigue characteristics on burring and tapping of ultra high strength TRIP steel sheet with Bainitic Ferrite Matrix

Akihiko Nagasaka[1)], Shunsuke Moriya[2)], Takahiro Nakazawa[3)], Koh-ichi Sugimoto[4)], Toshio Murakami[5)] and Tomohiko Hojo[6)]

[1), 2), 3)] *Nagano National College of Technology, 716 Tokuma, Nagano, Nagano 381-8550 Japan*
[4)] *Shinshu University, 4-17-1 Wakasato, Nagano, Nagano 380-8553 Japan*
[5)] *Material Design Research Section, Material Research Laboratory, Kobe Steel, Ltd., 1-5-5 Takatsukadai, Nishi-ku, Kobe, Hyogo 651-2271 Japan*
[6)] *Tsuyama National College of Technology, 624-1 Numa, Tsuyama, Okayama 708-8509 Japan*
[1)] nagasaka@nagano-nct.ac.jp

ABSTRACT

The effect of fatigue Characteristics on burring and tapping of 0.2C-1.5Si-1.5Mn (mass%) ultra high strength TRIP-aided steel sheets with bainitic ferrite matrix (TBF steel sheet) austempered at 375 or 450°C, was investigated for automotive applications. The temperature around martensite start temperature (M_S) was applied as austempering temperatures. M_S of the TBF steel sheet was estimated as 420°C.
Holes of 5.3 mm diameter for constant stress fatigue test were produced by thermal drilling and tapping and the fatigue life was evaluated by measurement of number of cycle to failure. The combined rotational and downward force of the thermal drilling tool bit created friction heat. The height of the bushing was roughly 3 to 4 times the initial sheet thickness. The bushings are ideal for thread applications, as the strength of threads was significantly increased. In TBF steel sheet, TBF steel sheet austempered at 375°C showed higher fatigue life than that of 450°C. Compared to TBF steel sheet austempered at 450°C, the burring and tapping contributed to the improvement of the fatigue limit to 1 100MPa with TBF steel sheet austempered at 375°C possessing fine bainitic ferrite matrix.

Keywords: TRIP Steel Sheet, Burring, Tapping, Fatigue Properties

---

[1), 4)] Professor
[2), 3)] Student
[5)] Senior Researcher
[6)] Lecturer
Note: Copied from the manuscript submitted to “Steel and Composite Structures, An International Journal” for presentation at ASEM13 Congress

1. INTRODUCTION

In recent years, it is expected to make use of high strength low alloy TRIP steel sheet, which has superior press formability, as various members for hybrid and electric cars [1)-5)]. To date, researches on burring of TRIP steel sheet have been reported [6)-7)], but reports on the effect of burring of the TRIP steel sheet are not sufficient.
In this research, we have aimed (nutless) improvement in burring TRIP steel sheets, and investigated effect of burring and tapping on various TRIP (TBF) [8)] steel sheets with bainitic ferrite matrix.

2. EXPERIMENTAL PROCEDURE

We used cold rolled steel sheets (thickness: 1.2 mm) that contain a chemical composition shown in Fig. 1. We processed austempering (γ) at 375 or 450°C for 200 s after austenite at 950°C for 1200 s. After that, we named such steels TBF375 and TBF450 respectively. At this point, we have used the temperature before or after the (420°C) M_S point of TBF steel for austempering temperature.
We found M_S point by following equation [5)].

$$M_S(°C) = 550 - 361×(\%C) - 39×(\%Mn) - 0×(\%Si) + 30×(\%Al) - 5×(\%Mo) \quad (1)$$

For comparing, we prepared polygonal ferrite TRIP steel sheets (TDP) which are processed austempering at 400°C for 1000 s after annealing second phase at 780°C for 1200 s. Incidentally, amount of Mn and Si addition are almost constant in TDP steels, we changed amount of carbon adding in the range of 0.1 to 0.4 mass%. Further we used ferrite and martensite composite structure steel (MDP) which doesn't contain retained austenite (γ_R).

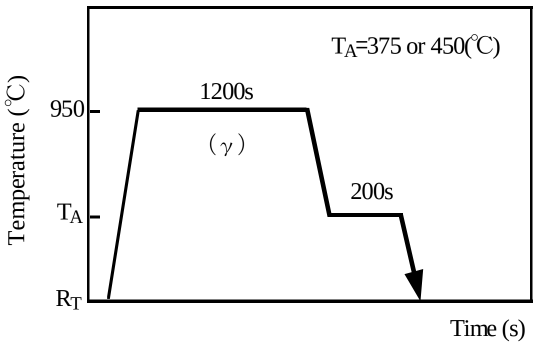

Fig. 1. Heat treatment diagram of TBF steel.

Table 1. Chemical composition (mass%) of steel used.

steel	C	Si	Mn	P	S	Al
TBF	0.20	1.51	1.51	0.015	0.0011	0.040
TDP1	0.10	1.49	1.50	0.015	0.0012	0.038
TDP2	0.20	1.51	1.51	0.015	0.0011	0.040
TDP3	0.29	1.46	1.50	0.014	0.0012	0.043
TDP4	0.40	1.49	1.50	0.015	0.0012	0.045
MDP	0.14	0.21	1.74	0.013	0.0030	0.037

Fig.2 shows burring and tapping test equipment. We used MC (machining center) as the testing machine. We used the plate specimen (150×50 mm) and put M6 short flow drill (diameter=5.3mm) and cut at cutting feed speed *F*=10mm/min, revolution speed *n*=3500rpm.After that, we tapped and carried out fatigue test as needed (stress rate *R*=0.1 (Tensile-Tensile, Pulsating) frequency: 10Hz, sine wave, maximum stress σ_{max}=400 MPa, minimum stress σ_{min}=40 MPa). In addition, we measured spindle load meter Z axis load meter (thrust equivalent) *S* and of (torque equivalent) *T*.
In the tensile test, using JIS-13B type tensile specimen (Fig. 3) manufactured on the rolling direction, we tested (gage length: *GL*=50 mm, average strain rate: 2.8×10^{-4} /s) at 1mm/min crosshead speed.

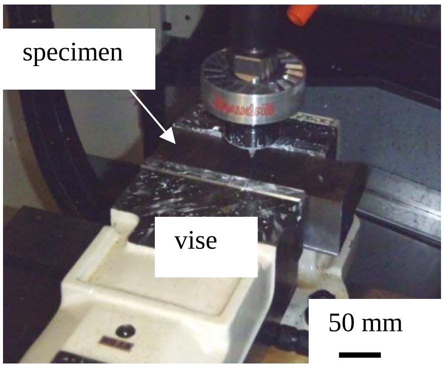

Fig. 2. Burring and tapping test equipment.

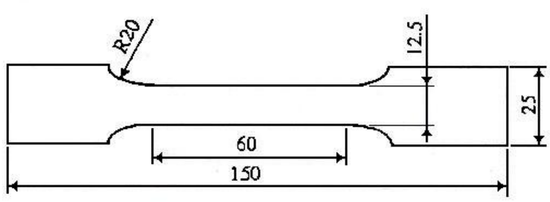

Fig. 3. JIS-13B type tensile specimen.

We found initial volume fraction ($f_{\gamma 0}$) in γ_R by using five-peak method ((200)α, (211)α, (200)γ, (220)γ and (311)γ) of X-ray diffraction analysis (Mo-Kα line). Moreover, we calculated initial carbon concentration $C_{\gamma 0}$ (mass%) in γ_R by substituting lattice a_γ (nm) constant that was found diffraction surface on Cr-Kα line, into following equation[9].

$$C_{\gamma 0} = (a_\gamma - 0.35467) / 4.67\times10^{-3} \quad (2)$$

3. RESULTS AND DISCUSSION

3.1 Microstructure and Tensile Properties

Fig. 4 shows micrograph of TBF steel. Fig. 4(a) shows microstructure of TBF375, and Fig. 4(b) shows microstructure of TBF450. White parts are γ_R or martensite (α_m) and gray parts are bainitic-ferrite (α_{bf}). Further, Table 2 shows the second-phase of specimen after the heat treatment, γ_R property and tensile property. The microstructure of TBF375 austempered at 375 degrees less or equal to *Ms* point (420℃) of TBF steel, consists mostly of α_{bf} and γ_R. The most part of γ_R exists as film state. On the other hand, TBF450 austempered at 450 degrees also consist of α_{bf} in the parent phase, and the γ_R and 8.1 vol% α_m exist in the second phase. At this time, initial volume fraction of $f_{\gamma 0}$ of γ_R in TBF450 increased compared with TBF375 [2]. Further, the tensile strength *TS* of TBF350 has 1 100MPa *TS* higher than TBF450.
Fig. 5 shows the microstructure of TDP2 steel. Second phase that consists of residual austenite (γ_R) and bainite (α_b), exist polygonal-ferrite in parent material.

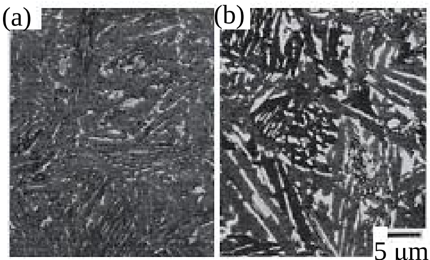

Fig. 4. Micrograph of TBF steel. ((a) TBF375, (b) TBF450) (white:γ_R or α_m, gray:α_{bf})

Table 2. Retained austenite characterisics and tensile properties of steel sheets used. heat treatment, γ_R property and tensile characteristics

steel	T_A (℃)	f (vol%)	$f_{\alpha m}$ (vol%)	$f_{\gamma 0}$ (vol%)	$C_{\gamma 0}$ (mass%)	YS (MPa)	TS (MPa)	UEl (%)	TEl (%)	RA (%)
TBF375	375	8.9	0	8.9	1.16	971	1154	4.4	7.8	40.3
TBF450	450	19.3	8.1	11.2	0.96	617	918	14.2	18.2	44.5
TDP1	400	19.9	0	4.9	1.31	429	651	27.8	37.2	49.2
TDP2	400	35.3	0	9.0	1.38	526	825	31.7	36.0	44.0
TDP3	400	44.1	0	13.2	1.41	562	895	28.6	32.2	41.8
TDP4	400	55.1	0	17.0	1.45	728	1103	29.2	32.8	41.8
MDP	-	27.1	27.1	-	-	593	783	8.3	13.1	44.5

T_A : austempering temperature, f, $f_{\alpha m}$, $f_{\gamma 0}$: intial volume fraction of second phase, martensite and retained austenite, $C_{\gamma 0}$: initial carbon concentration in retained austenite, YS : yield stress, TS : tensile strength, UEl : uniform elongation, TEl : total elongation and RA : reduction of area.

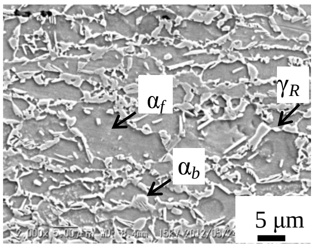

Fig. 5. Microstructure in TDP2 steel. (α_f: ferrite γ_R: retained austenite, α_b: bainite)

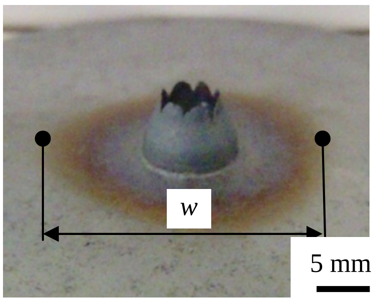

Fig. 6. Appearance after burring (w: Heat-affected width).

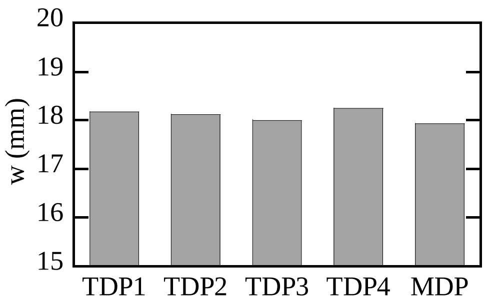

Fig. 7. Heat-affected width (w).

Fig. 8 shows relation between time (t) and burring load meter (TDP2 steel, F=10 mm/min, n=3500 rpm, D= 5.3 mm). Thrust (S) decreased as processing time of burring, then became maximum thrust S_{max}, raised later. On the other hand, torque T became maximum T_{max} later than S, and decreased after that.

Fig. 9 shows relation between tensile strength (*TS*) maximum thrust (S_{max}) and maximum torque (T_{max}). Because S_{max} value is approximately 20% and T_{max} value is approximately 15% regardless of the value of *TS*, it didn't indicate correlation between *TS* and S_{max} and T_{max}. Further, MDP steel that doesn't contain γ_R, indicates the same trend. We consider it was because of the moderate influence of processing-heat by flow-drilling.
Fig.10 shows a cross section of SEM micrograph after burring. Fig. 10(a) shows the cross section, Fig. 10(b) shows 0.3mm inside from the end face. At near the end surface, the void generated by punching isn't found (Fig. 10(a)).It is apparent that plasticity-flowing is large at 0.3mm internal (Fig. 10(b)).
Fig. 11 shows the flange portion schematic diagram. *H* is the burring height. We decided that thickness of reverse face of specimen is x_1, and x_2, x_3 to 1mm distance from reverse face to measure the flange thickness.
Fig.12 shows relation between each specimens and burring height *H*. It isn't indicated appreciable change about *H* in comparison from TDP1 to TDP4 steel, we consider that carbon additive amount doesn't affect *H* value. On the other hand, MDP steel became big approximately 1 mm in comparison with TDP steel.

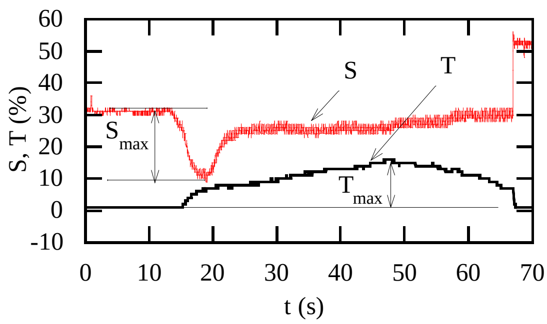

Fig. 8. Relation between time (*t*) and burring load meter (TDP2).

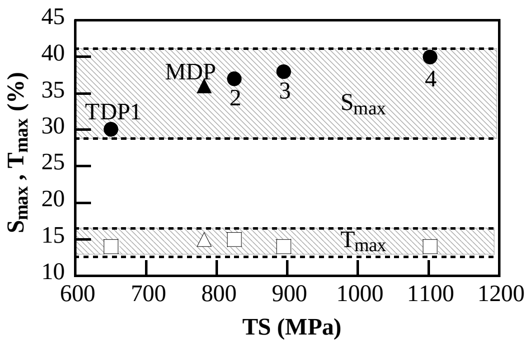

Fig. 9. Relation between tensile stress (*TS*) and maximum thrust (S_{max}) and aximum torque (T_{max}).

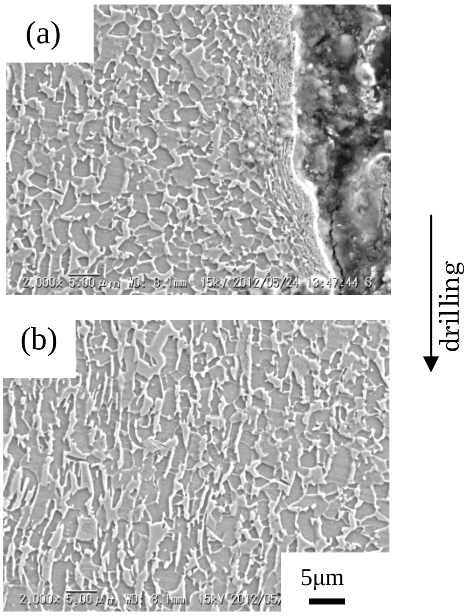

Fig. 10. Scanning electron micrographs of cross section after burring (TDP2 steel, (a) End face, (b) Location of 0.3 mm from the end face).

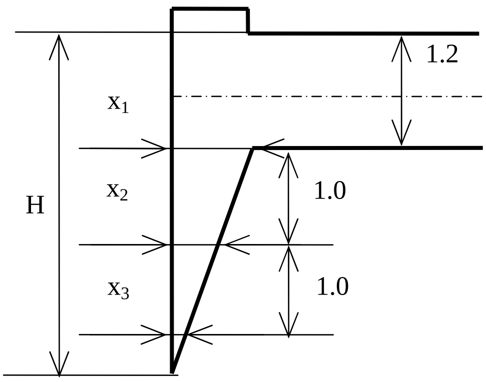

Fig. 11. Flange portion schematic diagram

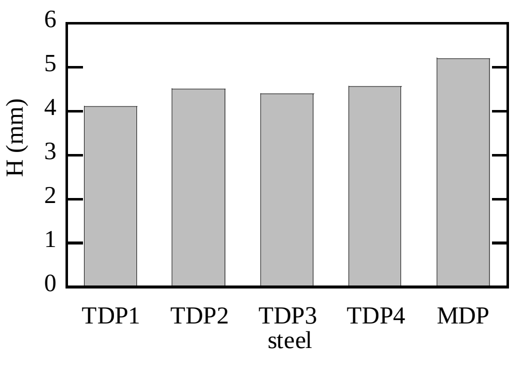

Fig. 12. Relation between burring height (*H*)

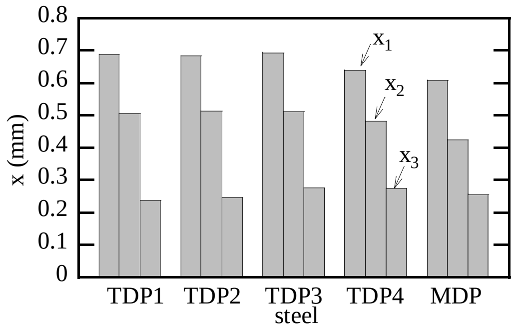

Fig. 13. Relation between flange thickness (x) and each specimens.

Fig.13 shows relation between flange thickness x and each specimens. Flange thickness x_1, x_2, x_3 are little different to compare from TDP1 to TDP4. On the other hand, x_1, x_2 of MDP steel became small when TDP4 and MDP steel are compared. From them, TDP steel's burring height H becomes smaller, however x becomes thicker in comparison with MDP steel, and because of this the flange part of TDP steel doesn't crack easily.

Fig.14 shows schema of Hardness of the flange part. We decided the base point 7 at 0.3 mm from burring-end face on center line in board thickness, and carried out Vickers hardness test to total 12 points in 0.3 mm intervals to base material direction and burring downward direction (Load: 0.98 N, Retention time: 5 s).

Fig.15 shows the distribution of Vickers hardness test after burring. From the distribution of HV of TDP2 steel, it is found that HV becomes higher from the vicinity of 6.We consider that it was caused by the strain induced transformation and work hardening by burring.

Fig.16 shows hardness increment ΔHV ($\Delta HV = HV_{\mathrm{max}} - HV_0$) of TDP steels and MDP steel. We named base material hardness HV_0 and the average of 9 to 12 HV is maximum hardness (HV_{max})after transformation. ΔHV increased as carbon additive amount increased in comparison from TDP1 to TDP4 (Fig. 16).We consider that it was affected of acted great on TRIP effect by virtue of increasing valid carbon concentration $f_{\gamma 0} \times C_{\gamma 0}$ which is consisted of the multiplication of initial carbon concentration $C_{\gamma 0}$ and initial volume rate $f_{\gamma 0}$ in γ_R by carbon additive amount increasing. In addition, comparing the MDP steel and TDP steel, we find that ΔHV of TDP steel is relatively large. We consider that MDP steel produced work-hardening following processing-heat at burring, and TDP steels is affected strain-induced-transformation ancillary to it.

Fig.17 shows relation between Vickers hardness HV and valid carbon concentration $f_{\gamma 0} \times C_{\gamma 0}$.At this point, we decided to name base material the HV_0,and average HV of 9 to 12 the maximum hardness HV_{max} after transformation. Comparing the TDP1 to TDP4 steel, ΔHV increases as carbon additive amount increases (Fig. 17).

Fig.18 shows number of cycles to failure N_f of each specimens after tapping. We excluded TDP4 steel because TDP4 was impossible to tapping.TBF375 steel indicates high fatigue life in comparison with TBF450 steel and TDP2 steel. N_f of TDP1 to TDP3 steel and MDP are approximately 1.5×10^5 cycles, and not different of N_f in each steels.

Fig.19 shows number of cycles to failure N_f of TDP2 that was processed differently. Further Fig.20 shows relation between crack length $2c$ and fatigue number of repetitions N. It is found that N_f is improved from drilling, burring and tapping in order (Fig.19).Crack generation delayed from drilling, burring and tapping in order. It is found that crack progressed at an accelerated pace after generated the crack on each processing (Fig. 20).We consider that it is caused by processing-affected-phase which was generated by burring. Moreover, we consider that it is caused by removal processing-affected-phase by tapping.

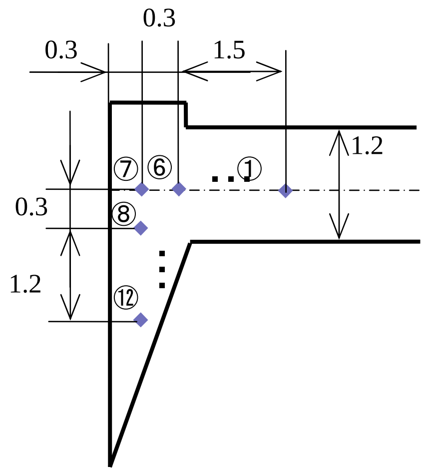

Fig. 14. Schema of Hardness of the flange part

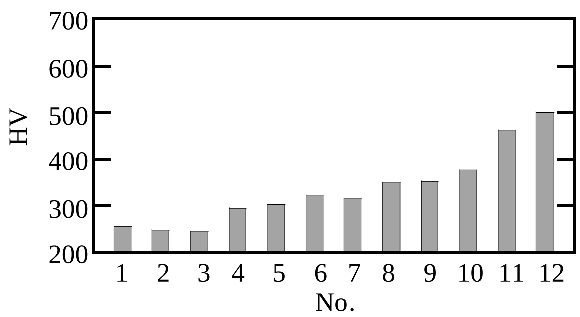

Fig. 15. Distribution of Vickers hardness (*HV*) after burring

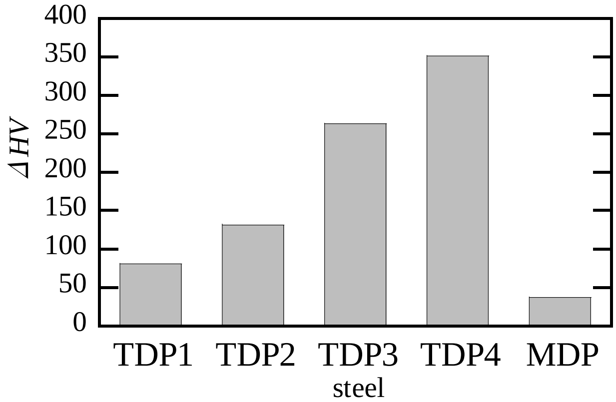

Fig. 16. Vickers hardness increment (*ΔHV*).

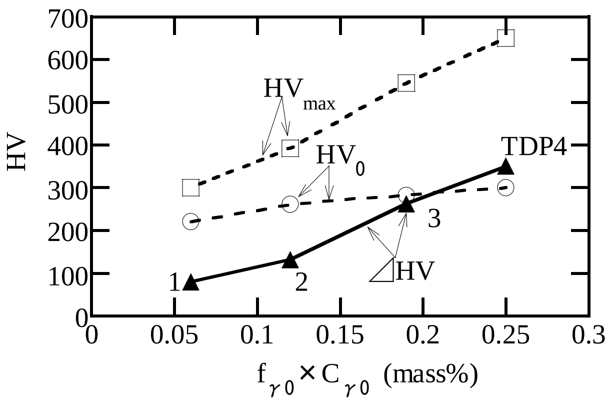

Fig. 17. Relation between Vickers hardness (*HV*) and total carbon concentration ($f_{\gamma 0} \times C_{\gamma 0}$).

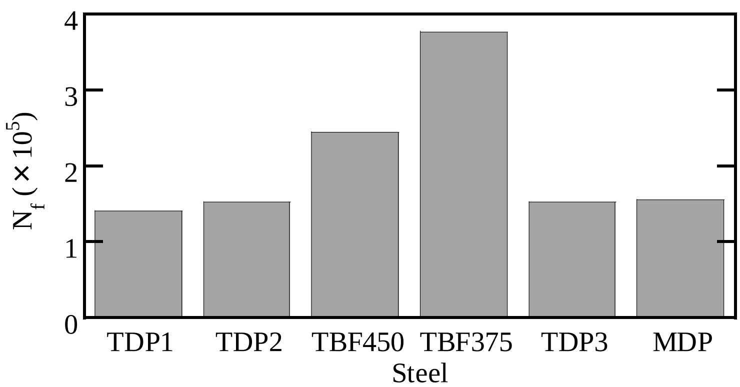

Fig 18. Number of cycle to failure (N_f) of each specimens after tapping

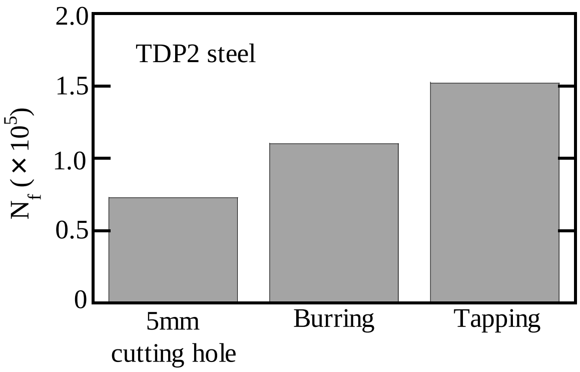

Fig. 19. Number of cycle to failure (N_f) of TDP2 steel that was processed different.

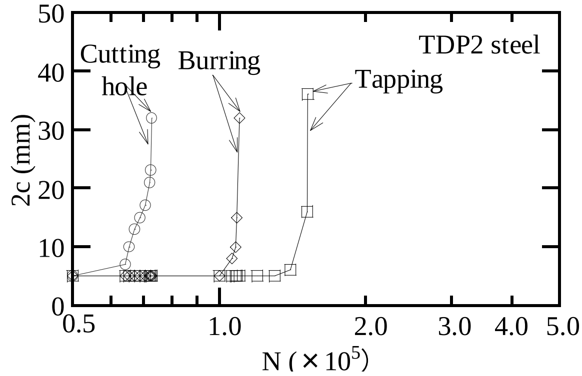

Fig. 20. Relation between crack length (2*c*) and number of cycles (*N*)

4. CONCLUSIONS

We investigated burring processing conditions on 1100MPa class ultra-high strength TRIP steel and the fatigue property. The results are as follows.

1) TBF375 steel after tapping showed a high fatigue life in comparison with TDP2 steel and TBF450 steel.
2) In TDP steel, maximum Vickers hardness HV_{max} of the flange after burring , and the incremental hardness

ΔHV are increased as carbon additive amount increased. We consider that it is caused of TRIP effect through the higher the total carbon concentration ($f_{\gamma 0} \times C_{\gamma 0}$) by the carbon additive amount increased.

3) After burring TDP1 to TDP3 steel and MDP steel are possible to tapping.
4) The carbon additive amount of TDP steel doesn't affect fatigue life after tapping great.
5) Burring of TDP inhibits fatigue crack generation.

We consider that caused by contributed processing-affect-phase in near the hole by burring.

6) Tapping inhibits fatigue crack generation greater than burring. We consider that processing-affect-phase generated by burring was removed moderately.

ACKNOWLEGEMENTS

The authors wish to thank Osawa Scientific Studies Grants Foundation and Suzuki Foundation for their financial supports.

REFERENCES

1) K. Sugimoto, A. Nagasaka, M. Kobayashi and S. Hashimoto: ISIJ Int., 39 (1999), 56.
2) K. Sugimoto, S. Song, J. Sakaguchi, A. Nagasaka and T. Kashima : Tetsu-to-Hagane, 91 (2005), 278.
3) K. Sugimoto, A. Kanda, R. Kikuchi, S. Hashimoto, T. Kashima and S. Ikeda: ISIJ Int., 42 (2002), 910.
4) H. Hayashi, K. Tezen and T. Amaike : J. Jpn. Soc. Technol. Plast., 27 (1986), 984.
5) I. Tamura: Steel Material Strength, Nikkan Kogyo Shimbum, Tokyo, (1970), 39.
6) A. Nagasaka, S. Hasebe, A. Nakamura, T. Matsushima, K. Sugimoto and T. Murakami: Proc. of SHSS2010, CD-ROM, (2010).
7) Nagasaka et al.: J. of Iron and Steel Research, Int., 18 (2011), 44.
8) A. NAGASAKA, Y. KUBOTA, K. SUGIMOTO, A. MIO, T. HOJO, K. MAKII, M. KAWAJIRI and M. KITAYAMA: ISIJ International, Vol. **50** (2010), 1441.
9) H. Maruyama: J. Jpn. Soc. Heat Treat., **17** (1977), 198.
10) Z. Nishiyama: Martensite Transformation, Maruzen, Tokyo, (1979), 13.